Journal of Visualization, Vol. 6, No. 2 (2003) 125-133

Laser Flow Visualization and Velocity Fields by Particle Image Velocimetry in an Electrostatic Precipitator Model

Mizeraczyk , J.*[1], Dekowski, J.*[1], Podliński, J.*[1], Kocik, M.*[1], Ohkubo, T.*[2] and Kanazawa, S.*[2]

*1 Center of Plasma and Laser Engineering, Institute of Fluid Flow Machinery, Polish Academy of Sciences, 80–231 Gdańsk, Fiszera 14, Poland, E–mail: jmiz@imp.gda.pl
*2 Department of Electrical and Electronic Engineering, Oita University, 700 Dannoharu, Oita 870–1192, Japan.

Received 12 June 2002
Revised 9 September 2002

Abstract : Although improving electrostatic precipitator (ESP) collection of fine particles (micron and submicron sizes) remains of interest, it is not yet clear whether the turbulent flow patterns caused by the presence of electric field and charge in ESPs advance or deteriorate fine particle precipitation process. In this paper, results of the laser flow visualization and Particle Image Velocimetry (PIV) measurements of the particle flow velocity fields in a wire–to–plate type ESP model with seven wire electrodes are presented. Both experiments were carried out for negative and positive polarity of the wire electrodes. The laser flow visualization and PIV measurements clearly confirmed formation of the secondary flow (velocity of several tens of cm/s) in the ESP model, which interacts with the primary flow. The particle flow pattern changes caused by the strong interaction between the primary and secondary flows are more pronounced for higher operating voltages (higher electrohydrodynamic number N_{EHD}) and lower primary flow velocities (lower Reynolds number Re). The particle flow patterns for the positive voltage polarity of the wire electrodes are more stable and regular than those for the negative voltage polarity due to the nonuniformity of the negative corona along the wire electrodes (tufts).

Keywords : Flow visualization, Electrostatic precipitator, PIV, Corona discharge, EHD flow.

1. Introduction

In recent years a special environmental concern is directed towards controlling the emission of micron and submicron particles in electrostatic precipitators (ESPs), which operating with high overall efficiency, are not effective in the removal of fine particles. Many of the fine particles of 1 μm or less in size contain toxic trace elements. Hence, there has long been interest in improving ESP collection of fine particles.

The motion and precipitation of particles in the duct of an ESP depend on the particle properties, electric field, space charge and gas flow field. It was shown (Ohkubo et al., 1986; Atten et al., 1987; Medlin et al., 1998; Chang and Bai, 2000; Mizuno, 2000; Mizeraczyk et al., 2001; Yamamoto et al., 2002) that a significant interaction between these factors exists, resulting in significant turbulent flow patterns in the ESP. However, it is not yet clear whether these turbulent flow patterns advance or deteriorate fine particle precipitation process. To elucidate the influence of the electrically generated flow disturbances on the precipitation of fine particles in ESPs, more experimental investigations are needed.

In this paper, results of the laser flow visualization and Particle Image Velocimetry (PIV) measurements of the particle flow velocity fields in a wire–to–plate type ESP model with seven wire electrodes are presented. This investigation is expected to be helpful in elucidating the motion of the fine particles in ESPs.

2. Experiment

The apparatus used in this experiment consisted of an ESP model, a laser flow visualization set–up and standard PIV equipment for the measurement of velocity field (Fig.1).

The ESP model was a transparent plane–parallel acrylic duct, 160 cm long, 20 cm wide and 10 cm high. In the middle of the ESP model, seven stainless–steel wire electrodes (diameter of 0.1 cm, length of 20 cm, 10 cm apart from each other) were mounted in the acrylic side–walls, parallel to the opposite facing stainless–steel plate collecting electrodes. The distance between the collecting electrodes (110 cm long and 20 cm wide) was 10 cm.

The applied voltage, either negative or positive, was varied from that of the corona onset up to 30 kV, which corresponds to a mean electrostatic field strength of 6.0 kV/cm at the wire electrode (no discharge). The voltage was supplied to each wire electrode through a 10 MΩ resistor. Air seeded with cigarette smoke (size of less than 1 μm, in dry air) was blown along the ESP duct with an average velocity ranging from 0.14 to 0.60 m/s (a flow velocity of about 0.8 m/s is typical of ESPs). Some measurements were carried out under stationary conditions, without any externally forced movement of the air in the duct.

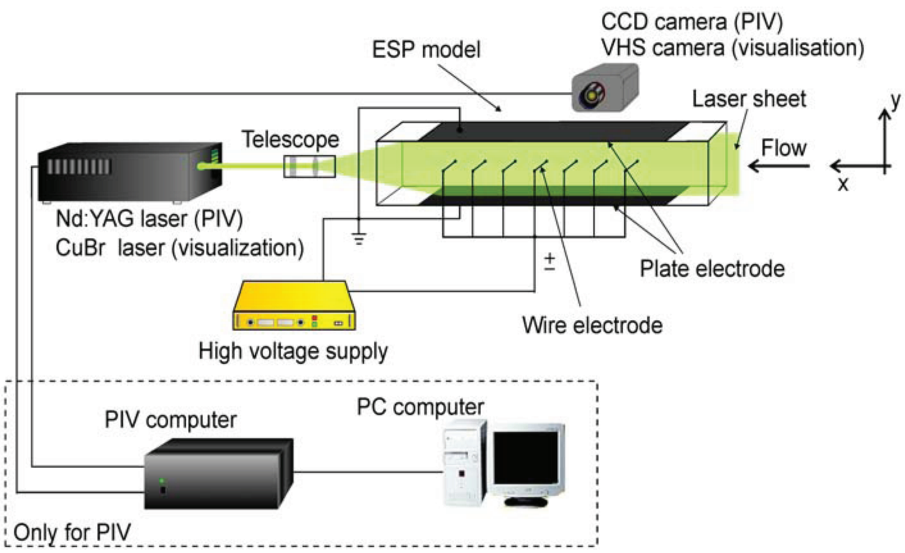

Fig. 1. Experimental set–up.

The laser flow visualization set–up consisted of a pulsed CuBr laser (λ = 510.6 and 578.2 nm) used as a light source, a cylindrical telescope to transform the CuBr laser beam into a laser sheet (1 mm thickness) passing along the ESP model and a video–camera for recording the flow patterns revealed by the laser sheet in the ESP model. The CuBr laser is a convenient light source for flow pattern observation and recording because of the high brightness of its beam (pulse energy of about 1 mJ) and its relatively high repetition rate (about 20 kHz).

The PIV equipment consisted of a twin second harmonic Nd–YAG laser system (λ = 532 nm, pulse energy 50 mJ), imaging optics (cylindrical telescope), CCD camera, image processor (Dantec PIV 1100) and PC computer (Mizeraczyk et al., 2001). A laser sheet of thickness of 1 mm, formed from the Nd–YAG laser beam by the cylindrical telescope was introduced into the ESP model, perpendicularly to the plate electrodes. The particle images were recorded by the Kodak Mega Plus ES 1.0 CCD camera, which could capture two images with a minimum time separation of 2 μs. The CCD camera active element size was 1008 × 1018 pixels. The captured images were transmitted by a Dantec PIV 1100 image processor to the PC computer for digital analysis.

The velocity field maps presented in this paper are composed of several adjacent velocity fields (from 4 to 9), each having an area of 10 x 10 cm. All of the presented velocity field maps resulted from the averaging of 100 measurements, which means that each presented velocity map is time–averaged.

3. Results

In the following text, the externally forced flow of the air (seeded with cigarette smoke particles) along the duct is called a primary flow (not influenced by the electric force), in contrast to the flow of the seed particles, which may not follow the primary flow when applying the voltage.

When the visualization or PIV method is used for the velocity field monitoring of the flow seeded with particles in which an electric force does not exist, the obtained velocity field pattern reflects the motion of the primary flow, assuming that the seed particles follow the flow. However, when an electric force exists in the flow, the seed particle motion depends not only on the primary flow motion, but is also influenced by the electric force. Therefore, the velocity field patterns monitored by both methods (visualization and PIV) in the ESP model reflect the motion of the seed particles, or, in general, particles present in the ESP model.

Therefore, the velocity field patterns presented in this paper describe the motion of the particles in the ESP model. However, the patterns measured without applied voltage also correspond to the primary flow motion.

3.1 Flow velocity field patterns

3.1.1 Stationary case – without primary flow

When applying the high voltage in the stationary case (i.e. without the primary flow), particle flow patterns develop around the electrode wires, and these differ for positive and negative voltage polarities. The time evolution of these patterns is shown in Figs. 2 and 4.

Positive voltage polarity

After applying the voltage, the seed particles are pushed from the wire electrodes outwards by the electric force which is strongest around the wires. The dark circular areas around the wire electrodes seen in Fig. 2 at t = 0.2 s and 0.4 s are the areas from which the particles have already been removed (the brightness of the image is proportional to the seed particle concentration). With elapsing time, "the particle removal wave" moves farther outward making the dark particle–free areas around the wire electrodes larger (t =0.5 s). After that time, uniformly dark particle removal areas break up. At first, bright "islands" appear in the dark particle removal areas. Then, the particle removal areas become irregular and turbulent.

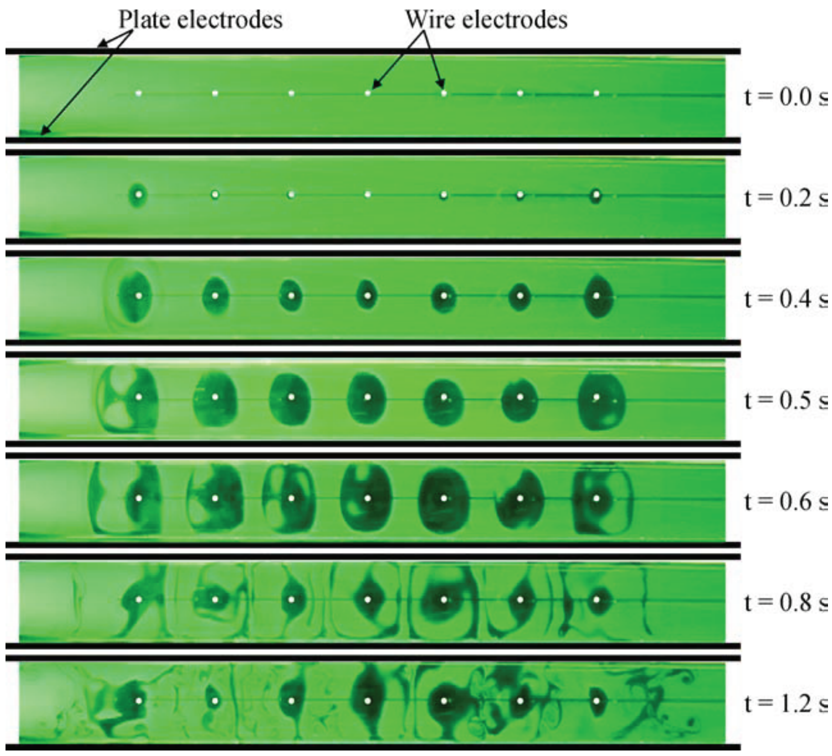

Fig. 2. CuBr laser visualization. Time evolution of the circular structures of the seed particle flow after applying high voltage at t = 0 without primary flow. Positive polarity, voltage 25 kV.

The uniformly dark, circular shape of particle removal areas observed just after applying the voltage (t = 0 – 0.4 s) show that the carrier gas (air) does not follow the electrically forced motion of the seed particles, exhibiting a motion inertia. However, the bright islands in the particle removal areas at time t = 0.5 – 0.8 s indicate that the electrically induced motion of the seed particles and ions has caused the carrier gas to move. This motion has transported the seed particles from other parts of the ESP into the dark particle removal areas, resulting in the clouds of seed particles which, due to the light scattering, are seen as the bright islands in the dark particle removal areas. With elapsing time, the relation between the seed particle removal by the electric force away from the wire electrodes and the increasing seed particle transport by the carrier gas towards particle–free areas around the wire electrodes becomes chaotic. This results in the irregular and turbulent flow patterns of the seed particles, as seen at t > 1 s (Fig. 2). However, despite the generally chaotic motion of the seed particles at t > 1 s, the dark, particle–free areas are clearly present in the vicinity of the wire electrodes, indicating strong removal of the seed particle away from the wire electrodes.

Figure 3 shows the particle flow pattern and time–averaged velocity field around the second wire electrode (counting from the ESP model inlet) at t = 1 s after applying the high voltage (17 kV). Since the operating voltage is lower than that in Fig. 2, the circular removal wave of the seed particles is still well-preserved regardless of a relatively long time elapsing after applying the voltage. The vectors at the left side in Fig. 3, directed towards the wire electrode, illustrate the motion of the particles caused by the electric field from the adjacent wire electrode.

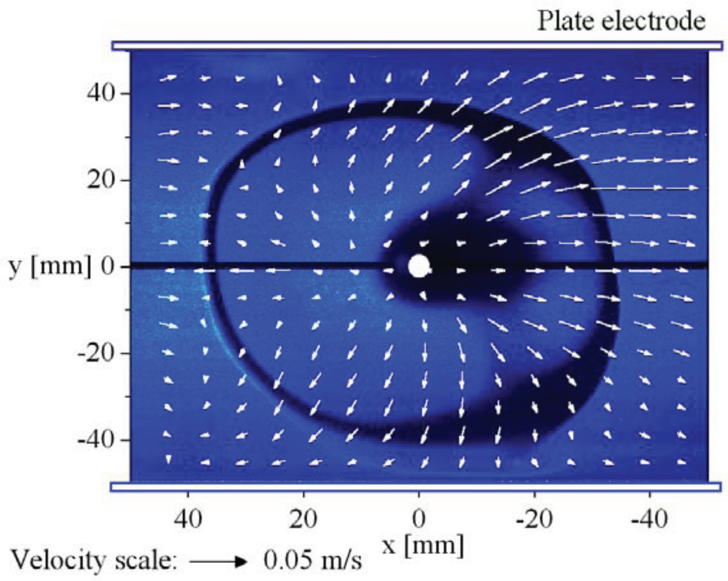

Fig. 3. Image of the seed particle flow pattern and velocity field around the second wire electrode in the ESP model without primary flow at t = 1 s after applying the high voltage. Positive polarity, voltage 17 kV.

Negative voltage polarity

At negative polarity, the particle flow pattern (Fig. 4) does not exhibit any regularity as it does just after applying the positive high voltage. The particle flow pattern at negative polarity is irregular and turbulent. The removal of the seed particles from the areas around the electrode wires is faster than in the case of positive polarity. At t = 1.2 s after applying the voltage, the area around the wire electrodes is almost dark, indicating low concentration of the seed particles.

The more turbulent character of the flow patterns at negative voltage polarity is probably due to nonuniformity of the negative corona discharge, which exhibits the form of tufts irregularly in time and space distributed along the wire (Schwabe et al., 1988). Around the tufts, small three–dimensional flow structures occur. They not only interact with each other, but even disappear when the tufts move or vanish. As a result, we observe stochastically distributed flow fluctuations, which we call flow turbulence.

3.1.2 Dynamic case – with primary flow

Positive voltage polarity

The particle velocity field patterns in the ESP model for two different velocities of the primary flow (0.14 m/s and 0.6 m/s) at constant positive voltage of 24 kV are shown in Figs. 5 and 6, respectively. They confirm existence of strong secondary flows of the seed particles, caused by the electric field and charge. The secondary flow patterns depend on the applied voltage and the velocity of the primary flow.

At a relatively low primary flow velocity of 0.14 m/s (i.e. at a moderate Reynolds number Re = 460) and an operating voltage of 24 kV (i.e. at a high electrohydrodynamic number N_{EHD} = 28), strong vortexes are formed in both the upstream and downstream regions of the ESP duct (Fig. 5). In this case, the electric force dominates over the inertial one. N_{EHD} number is the ratio of the conductive electric Rayleigh number to Reynolds number squared (Chang and Watson, 1994).

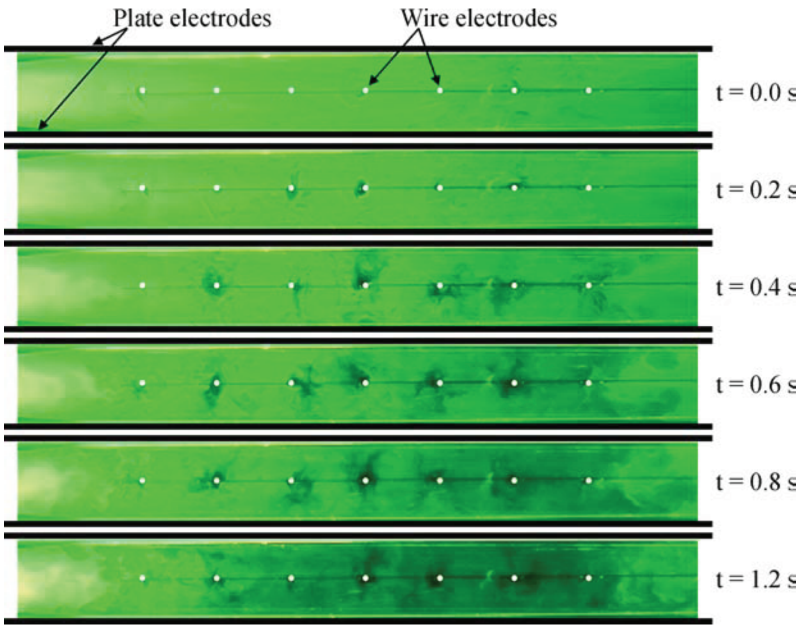

Fig. 4. CuBr laser visualization. Time evolution of the circular patterns of the seed particle flow after applying the high voltage at t = 0 s without primary flow. Negative polarity, voltage 25 kV.

Increase in the primary flow velocity diminishes the influence of the electric force on the particle motion – the vortexes disappear, eventually resulting in the primary-flow-dominated velocity field pattern of the seed particles (Fig. 6, the primary flow velocity 0.6 m/s, Re = 2000, N_{EHD} = 1.7). At higher primary flow velocities, the precipitation of the seed particles is not as efficient as at a lower primary flow velocity (e.g. at 0.14 m/s, Fig. 5) due to higher seed particle mass flow rate, shorter residence time and weaker influence of the electric field. As a result the seed particles are present in the primary flow after passing through all seven wire electrodes, making the PIV measuring possible along the whole duct of the ESP model (compare Fig. 5, where the PIV measuring was not possible beyond the third electrode due to the strong particle precipitation).

We found that the electric field influence on the particle velocity field pattern also become stronger at higher operating voltages, resulting in stronger coherent vortex structures, in the upstream region of the ESP model duct (see the vortexes around 60 mm from the first wire electrode upstream in Fig. 5).

Negative voltage polarity

At negative voltage polarity, the time–averaged particle velocity fields are astonishingly similar to those at positive polarity shown in Figs. 5 and 6 (hence the velocity fields at negative polarity are not presented in this paper). The secondary flow, formed at negative polarity, with apparent vortexes (as in Fig. 5 for positive polarity) is also more pronounced at lower velocities of the primary flow (because of the lower Re). The secondary flow weakens with increasing primary flow velocity, similar to positive polarity in Fig. 6.

At a lower primary flow velocity (less than 0.4 m/s), the seed particles are very quickly removed from the carrier gas already in the region of the first three wire electrodes, similarly as at positive polarity. Beyond the third wire electrode the flow is practically free from seed particles.

We found higher velocity fluctuations in the flow pattern at negative voltage polarity which are probably due to temporal and spatial fluctuations of the negative corona discharge.

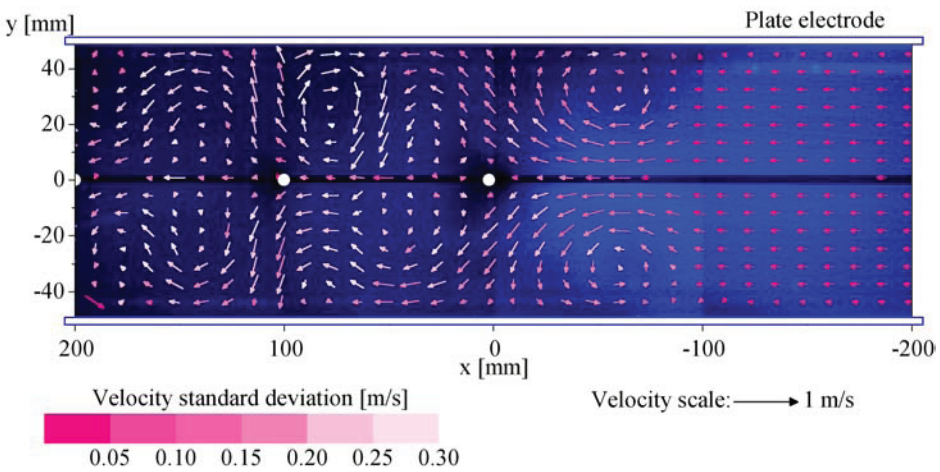

Fig. 5. Flow velocity field in the ESP model at a primary flow velocity of 0.14 m/s. Positive polarity, voltage 24 kV, Re = 460, N_{EHD} = 28. Only the flow patterns around there wire electrodes are shown (on the left side of the third wire electrode, the seed particles vanished due to efficient electrostatic precipitation).

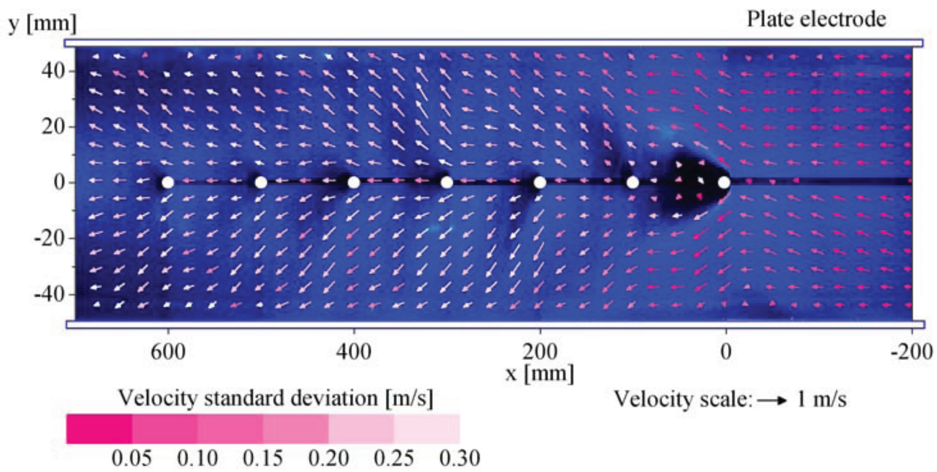

Fig. 6. Flow velocity field in the ESP model at a primary flow velocity of 0.6 m/s. Positive polarity, voltage 24 kV, Re = 2000, N_{EHD} = 1.7.

4. Conclusions

The presented results for the flow visualization and the PIV measurements of the particle velocity field in the ESP model confirmed that the presence of the electric field and charge causes a significant change in the particle flow pattern. After applying the voltage, secondary flow having velocity of several tens of cm/s is formed in the ESP model, interacting with the primary flow. This results in strong vortexes in the downstream and upstream regions of the ESP model duct, if the primary flow velocity is relatively low (below 0.4 m/s). The primary flow disturbances are more pronounced for lower primary flow velocities (low Reynolds number) and/or higher operating voltages (high electrohydrodynamic number). Under these conditions, the precipitation of the particles in the ESP model is high.

The flow patterns in the ESP model at positive voltage polarity are more stable and regular than those for the negative voltage polarity. The turbulence intensity is also smaller for the positive voltage polarity. The more turbulent character of the flow patterns at negative voltage polarity is probably due to nonuniformity of the negative corona discharge along the wire electrode, as exhibited by the tufts.

The presented velocity maps illustrate time–averaged two–dimensional velocity field of the seed particles in the selected (middle) longitudinal cross–section of the flow duct in the ESP model. This is the first step toward experimental investigation of the three–dimensional velocity field in the ESP model.

Acknowledgements

This research was sponsored by the Foundation for Polish Science (Fundacja na Rzecz Nauki Polskiej, subsidy 8/2001) and the State Committee for Scientific Research (KBN PB 1756/T10/01/21). Fruitful discussions with Prof. J.S. Chang are thankfully acknowledged.

References

Atten, P., McCluskey, F. M. J. and Lahjomri, A. C., The Electrohydrodynamic Origin of Turbulence in Electrostatic Precipitators, IEEE Transactions on Industry Applications, 23-4 (1987), 705-711.

Chang, C. L. and Bai, H., Effects of Some Geometric Parameters on the Electrostatic Precipitator Efficiency at Different Operation Indexes, Aerosol Science and Technology, 33-3 (2000), 228-238.

Chang, J. S. and Watson, A., Electromagnetic Hydrodynamics, IEEE Transactions on Dielectrics and Electrical Insulation, 1-5 (1994), 871-895.

Medlin, A. J., Fletcher, C. A. J. and Morrow, R., Electrohydrodynamic Modelling of Fine Particle Collection in Electrostatic Precipitators, Proc. of 7th International Conference on Electrostatic Precipitation (Pohang), (1998), 665-672.

Mizeraczyk, J., Kocik, M., Dekowski, J., Dors, M., Podliński, J., Ohkubo, T., Kanazawa, S. and Kawasaki, T., Measurement of the Velocity Field of the Flue Gas Flow in an Electrostatic Precipitator Model using PIV Method, J. Electrostatics, 51-52 (2001), 272-277.

Mizuno, A., Electrostatic Precipitation, IEEE Transactions on Dielectrics and Electrical Insulation, 7-5 (2000), 615-624.

Ohkubo, T., Nomoto, Y., Adachi, T. and McLean, K. J., Electric Field in a Wire-Duct Type Electrostatic Precipitator, J. Electrostatics, 18 (1986), 289-303.

Schwabe, R. J., Snaddon, R. W. L., Nelson J. K. and Salasoo, L., An Optical Study of Negative-Corona Tuft Distribution for Pulsed Electrostatic Precipitator Applications, J. Phys. D: Appl. Phys., 21 (1988), 546-551.

Yamamoto, T., Okuda, M. and Okubo, M., Three-dimensional Ionic Wind and Electrohydrodynamics of Tuft/Point Corona Electrostatic Precipitator, Proc. of 2002 IEJ Annual Meeting , Toyahashi, Japan, (2002), 105-112.

Author Profile

Jerzy Mizeraczyk: He received his M.Sc. in Electronics from the Technical University of Gdańsk in 1966, his Ph.D. from the Technical University of Gdańsk in 1976, and his Dr. hab. in Electrical Engineering from the University of Gdańsk in 1988. He was a fellow of the Japan Society for the Promotion of Science at Nagoya University, Japan, of the A. v.–Humboldt Foundation and of the H. Hertz Foundation at the Ruhr University Bochum, Germany. He was a Visiting Senior Researcher at the Chalmers University of Technology, Göteborg, Sweden, and at McMaster University, Hamilton, ON, Canada. He was a Full Professor at Oita University, Japan. He is currently Professor and Head of the Centre of Plasma and Laser Engineering, Institute of Fluid–Flow Machinery, Polish Academy of Sciences, Gdańsk, Poland. He was Co–Director of two European Community Copernicus Projects and NATO "Science for Peace Programme". He has worked in the areas of plasma physics, dc, pulsed, RF and MW discharges, lasers and their applications, and plasma chemistry for environmental technologies. He has authored more than 100 published refereed papers and has presented more than 100 conference papers on these topics.

Jarosław Dekowski: He received his M.Sc. degree in Applied Physics in the field of fluid mechanics at the Technical University of Gdańsk in 2002. He works as an Assistant Researcher at the Institute of Fluid Flow Machinery, Polish Academy of Sciences, Gdańsk, Poland. His research interests include fluid and particle flows in electrostatic precipitators, electrohydrodynamics, PIV measurement technique, and numerical fluid dynamics.

Janusz Podliński: He received his M.Sc. degree in Electronics and Telecommunications at the Technical University of Gdańsk in 2001. He works as an Assistant Researcher at the Institute of Fluid Flow Machinery, Polish Academy of Sciences, Gdańsk, Poland. His research interests include fluid and particle flows in electrostatic precipitators and non–thermal plasma reactors, electrohydrodynamics, and PIV measurement techniques.

Marek Kocik: He received his M. Sc. in 1996 from the University of Gdańsk in Experimental Physics in the field of atomic spectroscopy. He received his Ph.D. degree from the Institute of Fluid Flow Machinery, Polish Academy of Sciences in 2002, where he is presently an Associate Researcher. His research concerns laser applications to micromachining, laser flow diagnostics and laser spectroscopy. He has authored 15 published refereed papers and has presented more than 40 conference papers on these topics.

Toshikazu Ohkubo: He was born in Beppu, Japan, in 1948. He received B.E., M.E., and D.E. degrees from Kyushu University, Fukuoka, Japan, in 1972, 1975 and 1986, respectively. From 1975 to 1987 he was a Research Associate in the Department of Electrical Engineering, Oita University, Oita, Japan. From 1988 to 1989 he was a Visiting Research Fellow at McMaster University, Hamilton, ON, Canada. He become an Associate Professor in 1987 and a Professor in 1995 in the Department of Electrical Engineering, Oita University. His research interests include NO_x removal by corona discharge–induced plasmas, electrohydrodynamics, laser–induced fluorescence technique, and thin–film preparation by pulsed–laser deposition for fuel cells. He is a member of the Institute of Electrical Engineers of Japan, Institute of Electronics, Japan, and the Japan Society of Applied Physics.

Seiji Kanazawa: He was born in Usuki, Oita, Japan in 1961. He received B.E., M.E., and Ph.D. degrees from Kumamoto University, in 1985, 1987 and 1990, respectively. Since 1990, he has been with Oita University, Oita, Japan, where he is presently an Associate Professor in the Department of Electrical and Electronic Engineering. His research interests include applied electrostatics, air pollution control, plasma technologies, plasma diagnostics and eco–material processing using lasers. He is a member of the Institute of Electrical Engineers of Japan, the Institute of Electronics, Information, and Communication Engineers of Japan, the Institute of Electrostatics, Japan and the Japan Society of Applied Physics.